The H3K27me3 histone mark correlates with repression of colour and aroma development post-harvest in strawberry fruit

The H3K27me3 histone mark correlates with repression of colour and aroma development post-harvest in strawberry fruit.

Ashley Baldwin[1], Tamara Lechon[1], Angela Marchbank[1], Simon Scofield[1], Kerstin Lieu[1], Charlotte L. Wilson[1], Richard A. Ludlow[1], Robert J. Herbert[1,3], Hans-Wilhelm Nützmann[2], Hilary J. Rogers[1]*

[1]School of Biosciences, Cardiff University, Sir Martin Evans Building, Museum Avenue, Cardiff CF10 3AX, UK

[2]Biosciences, University of Exeter, Geoffrey Pope Building, Stocker Road, Exeter, EX4 4QD, UK

[3]School of Science and the Environment, University of Worcester, Henwick Grove, Worcester, WR2 6AJ, UK

Ashley Baldwin	BaldwinA@cardiff.ac.uk
Tamara Lechon	LechonGomezT@cardiff.ac.uk
Hans-Wilhelm Nützmann	H.Nuetzmann@exeter.ac.uk
Angela Marchbank	MarchbankAM@cardiff.ac.uk
Simon Scofield	ScofieldS@cardiff.ac.uk
Hilary Rogers	rogershj@cardiff.ac.uk
Kerstin Lieu	lieuK@cardiff.ac.uk
Charlotte Wilson	wilsonCL6@cardiff.ac.uk
Richard A. Ludlow	ludlowRA@cardiff.ac.uk
Robert J. Herbert	herbertR3@cardiff.ac.uk

HIGHLIGHT

A correlation is presented between the H3K27me3 histone mark and repression of a transcription factor cascade regulating colour and aroma development during dark chilled postharvest storage of strawberry fruit.

ABSTRACT

Strawberry ripening is non-climacteric, and post-harvest fruit enter senescence and deteriorate rapidly. Chilled storage induces transcriptome wide changes in gene expression, including the down-regulation of aroma related genes. Histone marks are associated with transcriptional activation or repression; the H3K27me3 mark is mainly associated with repression of gene expression. Here genes associated with H3K27me3 were identified through ChIP-seq in ripe red strawberry fruit at harvest and after 5 days of chilled storage in the dark. The number of ChIP peaks increased with storage time, indicating an increased role for this mark in regulation of gene expression following chilled dark storage. Comparing ChIP-seq data to RNA-seq data from the same material identified 440 genes whose expression correlates with H3K27me3 repression. Abiotic stress genes, especially cold stress response genes, were down-regulated during storage. Increased association with the H3K27me3 mark indicates that they may be repressed via this epigenetic mark. Other functional groups included cell wall and carbohydrate metabolism. The association with the H3K27me3 mark of two transcription factors (*FaHY5* and *FaTRAB1*) and *FaADH*, involved in ester biosynthesis, was validated by ChIP-PCR. These three genes are all down-regulated during storage and indicate a network of H3K27me3 gene repression affecting both anthocyanin and ester biosynthesis.

Keywords ChIP-seq; *Fragaria x ananassa*; fruit; H3K27me3; histone methylation; post-harvest; RNA-seq;

INTRODUCTION

Strawberry fruit develop from a single inflorescence as an aggregate fruit, where the receptacle comprises the main edible part of the fruit. This process involves structural, physiological and biochemical changes (Moya-León et al., 2019) resulting in an increase in sugar content, a change in fruit colour from green to red as well as secondary metabolite and aroma biosynthesis (Moya-León et al., 2019; Sánchez-Gómez et al., 2022; Kim et al., 2013). Strawberries are non-climacteric (Gu et al., 2019), therefore they do not increase their respiratory rate and are not responsive to ethylene post-harvest (Jia et al., 2011). Consequently, complete ripening occurs only on the plant and strawberry fruit are picked close to full maturity when they are in their final stages of ripening. Post-harvest, fruit initiates fruit senescence involving macromolecule breakdown, tissue softening and ending in cell death (Yun et al., 2012; Chen et al., 2014). As a result of this, they are highly perishable as they are less firm at harvest than climacteric fruit, increasing their susceptibility to mechanical damage and spoilage microorganisms (Siebeneichler et al., 2020). Post-harvest senescence is accelerated by respiration which is increased in wounded fruit as well as dehydration (Yang et al., 2014). Dehydration post-harvest also upregulates ABA signalling (Chen et al., 2014, 2016). This in turn promotes anthocyanin biosynthesis (Chen., 2016). During strawberry ripening this occurs through the activation of a transcription factor network involving TRAB1, MADS1 (Lu et al., 2023), HY5, RIF (Liu et al., 2023b; Li et al., 2020, 2023), and MYB10, (Medina-Puche et al., 2014). HY5 has also been shown to regulate post-harvest anthocyanin biosynthesis (Liu et al., 2023b). MADS1 has a role in repressing several aspects of strawberry fruit ripening. It represses several enzymes in the anthocyanin biosynthesis pathway as well as enzymes involved in cell wall modulation leading to softening, and the biosynthesis of important components of the strawberry aroma profile (Lu et al., 2023). Specifically, MADS1 represses the expression of AAT (acyl alcohol transferase). AAT is a key enzyme in ester biosynthesis, whose expression is down-regulated during chilled post-harvest storage of strawberry fruit (Baldwin et al., 2023). This correlates with changes in ester profile of the aroma. Esters are the major components of the strawberry aroma, and during 5 days of post-harvest storage at 8 °C the relative abundance of non-acetate esters in the aroma profile drops significantly (Baldwin et al., 2023).

Strawberry fruit have a short shelf-life post-harvest, especially when used in ready to eat fresh fruit salads, where they are also often halved. Hence in the commercial supply chain chilling is used to delay post-ripening senescence and reduce post-harvest spoilage from resident and opportunistic microflora (Feliziani and Romanazzi, 2016). Cold dark storage results in a transcriptomic and metabolic shift (Baldwin et al., 2023) down-regulating over 1000 genes including numerous transcription factors, and genes related to aroma biosynthesis. This shift in metabolism as a result of cold storage has been also reported in other soft fruit such as tomato (Zhang et al., 2016) where a down-regulation in the expression of flavour related genes was ascribed to promoter methylation. In *Fragaria vesca* DNA methylase and demethylase are highly expressed during fruit ripening, thus suggesting an involvement in regulation of gene expression (Gu et al., 2016). DNA methylation is also involved in regulation of senescence in other plant organs such as leaves (Yuan et al., 2020).

Other forms of epigenetic control have also been associated with plant organ senescence, including histone methylation (Zhang et al., 2022; Cigliano et al., 2022). Histone methylation can act to either repress or activate genes: for example, deposition of H3K4me3 and H3K36me3 marks is often observed on actively expressed genes, whereas H3K27me3 is often observed on repressed genes (Liu et al., 2010). In tomato, genome wide studies estimated that about half of the genes differentially expressed during post-harvest storage were epigenetically regulated, with a reduction in genes associated with the repressive histone mark H3K27me3 (Cigliano et al., 2022). H3K27me3 has also been shown in peach and apple to regulate ester formation, with H3K27me3 removal from NAC transcription factors and aroma related genes such as *AAT* (acyl alcohol transferase) increasing their expression during ripening (Cao et al., 2021). In strawberry, the genome-wide distribution of H3K9/K14 acetylation in the red-stage strawberry receptacles and H3K27me3 in red-stage fruits was used to characterise transcriptional regulation of expansin genes by histone modifications (Huang et al., 2020; Mu et al., 2021). Transcript levels of expansin genes were corelated with both histone marks suggesting that they are under epigenetic control in strawberry fruit. Interestingly, while H3K27me3 marks are typically enriched across the whole gene body (Cigliano et al., 2022; Liu et al., 2010; Payá-

Milans et al., 2019), Mu et al., (2021) showed H3K27me3 enrichment primarily at the 5' ends and promoters of two expansin genes in *F. vesca*.

Given the importance of epigenetic control both during senescence and post-harvest, the regulation of expression by the H3K27me3 mark was explored here in halved strawberries during a 5-day storage period where fruit were exposed to wounding followed by dark cold conditions. Using a genome wide ChIP-seq approach with a commercial strawberry cultivar we show that indeed a large number of genes are associated with both loss and gain of the H3K27me3 mark. Furthermore, our study suggests that this epigenetic regulator is involved in controlling both colour development and aroma production post-harvest in strawberries.

MATERIALS AND METHODS

Plant Material

Fragaria x ananassa cv. Elsanta plants were greenhouse grown at a minimum temperature of 19 °C with supplementary lighting (16 h). Harvested fruit were homogeneous in size, colour (at red ripe stage) with no external damage. They were immersed in 100 ml of 200 ppm sodium hypochlorite for 2 min, and air dried. The calyx was removed and fruits were halved: one half was processed immediately the other was stored for 5 days at 8 °C in a Jeiotech IL-21chilled incubator in the dark. Three replicates of three half fruits each were used per time point. Fruit were then skinned rapidly using a razor blade to remove all seeds and snap frozen in liquid nitrogen.

RNA-seq

RNA samples were extracted from fruit tissue (described above) following the protocol of Greco et al. (2014) and adapted by Dhorajiwala et al. (2021). RNA quality and concentration were verified by agarose gel electrophoresis, a Nanodrop spectrophotometer (Thermo Scientific) and an Agilent 2100 Bioanalyzer (Agilent). RNA was used for library preparation (poly A enrichment), tested using a Qubit 2.0 and an Agilent 2100 to test for concentration and insert size. Sequencing used an Illumina NovaSeq 6000, generating ≥ 40M paired-end reads per sample. Library preparation and sequencing

was performed by Novogene Co., Ltd. (Beijing, China). Sequences were quality checked and trimmed in house by Novogene Co., Ltd. (Beijing, China) and then aligned to the *Fragaria x ananassa* 'Royal Royce' Genome v1.0, (Hardigan et al., 2021) using HISAT2 v. 2.0.5 (Kim et al., 2019). A list of DEGs (P-adj <0.05, L2FC > 1 and < -1) was generated via DESeq2 (Love et al., 2014). For down-stream analyses, the transcriptome was compared to the *Fragaria vesca* Whole Genome v2.0.a1 Assembly & Annotation (Tennessen et al., 2014) via BLASTX.

Nuclear isolation, DNA fragmentation and Chromatin immunoprecipitation (ChIP)

Isolation of nuclei, DNA fragmentation and ChIP were according to Huang et al. (2020) starting with 2 g of frozen powdered fruit material. Nuclei were isolated by homogenization using a glass homogeniser (Kimble Chase, Ficher Scientific). Chromatin fragmentation used 30 U micrococcal nuclease (Thermo scientific, # EN0181) digestion optimised to a 10 min incubation time. ChIP was performed with native chromatin: Dynabeads Protein A (Thermo Fisher, cat. No 10001D) were used to pre-clear the digested chromatin and a H3K27me3 antibody (Sigma Aldrich, # 07-449) bound to Dynabeads was used to immunoprecipitate bound chromatin. DNA was recovered from the chromatin using a Monarch® PCR & DNA Cleanup Kit (New England Biolabs, #T1030S) alongside an input sample: fragmented chromatin that was not immunoprecipitated. Three biological replicates were used for each timepoint (day 0 and day 5 of chilled dark storage).

ChIP-seq

Immunoprecipitated DNA concentration was checked using a Qubit Fluorometer and DNA quality via a High Sensitivity D1000 ScreenTape (Agilent, #5067-5584). A NEXTflex™ Rapid DNA-Seq Kit (PerkinElmer # NOVA-5188) was used for paired-end DNA library construction. Sequencing used an Illumina® Next Seq 5000 Platform (120M reads per run) performed by the Biosciences Genomics Research Hub within the School of Biosciences, Cardiff University.

Low quality reads and sequencing adaptors were removed using Fastp (v0.20, Chen et al., 2018) and quality checked using Fastqc (v0.11.9) and MultiQC (v1.9, Ewels et al., 2016). Trimmed FASTQ reads were mapped using Bowtie2 (v2.4.1, Langmead and Salzberg 2012) using a maximum fragment length of 500 and the forward-reverse option to the three available genomes: *Fragaria x ananassa* 'Royal Royce' Genome v1.0 (https://www.rosaceae.org/Analysis/12335030, Hardigan et al., 2021), *Fragaria x ananassa* 'Camarosa' Genome Assembly v1.0.a1 (https://www.rosaceae.org/species/fragaria_x_ananassa/genome_v1.0.a1, Edger et al., 2019) and *Fragaria vesca* whole genome v2.0.a1 (https://www.rosaceae.org/species/fragaria_vesca/genome_v2.0.a1, Tennessen et al., 2014). The resulting Sequence Alignment/Map format (SAM) files were converted into Binary Alignment Map (BAM) format and sorted by chromosome using Samtools (v1.10). Using Samtools, Bamtools (v2.5.1) and Deeptools (v3.3.0), bigwig files (binSize = 50) were created to load into IGV (v2.12.3) to assess coverage. Peak calling was performed using MACS2 (v2.2.4, Zhang et al., 2008) with the broad calling argument (--broad -p 1e-3 -g 786543374). ChIPQC (v4.3, Carroll et al., 2014 within R v4.1.1) was used to assess sample quality. Following this analysis the two replicates with the highest quality for each time point were merged (Supplementary. Fig. S1), and the lowest quality replicate excluded from further analyses. This improved the quality scores: determined by the SSD and percentage of reads in peaks (RiP%) (Supplementary Table S1). Pseudo-replicates were created for both pull-down and input samples. Irreproducibility Discovery Rate (IDR v2.0.3) analysis using pseudo-replicate peak calls as well as non-pseudo-replicate peak calls was conducted to assess replicability. BEDTools (v2.29.2, Quinlan and Hall, 2010) intersect was used to find common peaks across pseudo-replicates. Coverage, peak length and the peak position were assessed using IGV. Diffbind (v3.17, Stark and Brown, 2011) was used to look for differences between storage time points (day 0 and day 5). ChIPseeker (v3.17, (Yu et al. 2015) was used for peak annotation and peak exploration. GO term enrichment was performed using PlantRegMap (Tian et al., 2020) and were visualised using the R package GOplot (Walter et al., 2015). IGV was used to visually assess the peak

quality. KEGG was also used to compare pathway changes between day 0 and day 5 of cold dark storage.

ChIP qPCR and RNA RT-qPCR

Total RNA extracted as above was DNase treated and cDNA was synthesised using the GoScript Reverse Transcription Mix, Oligo(dt) (Promega). Primers were designed using primer3 (http://primer3.ut.ee/; Rozen and Skaletsky 2000) and are listed in Supplementary Table S2. The real time qPCR (RT-qPCR) was conducted using a LightCycler® 96 instrument (Roche) and SyGreen Blue Mix Lo-ROX (PCR Biosystems Ltd., London, UK). Relative gene expression was quantified using the delta-delta Ct (2^DDCt) method (Livak and Schmittgen, 2001) using the gene encoding the small ribosomal subunit 40S as a reference gene (stable expression validated from the transcriptome data) For the ChIP validation, the percentage input method was used to calculate enrichment using 18S for validation (Supplementary Fig 2A). All PCR reactions were conducted using three biological replicates and two technical replicates.

Analysis of total anthocyanins

Strawberry fruit (*Fragaria x ananassa* cv. Elsanta) were harvested at red ripe stage and subjected to 5 days either at 8 °C in the dark in a Jeiotech IL-21chilled incubator or at 20 °C in the light (150 µmol/m^2/s). Fruit were processed as described above and 0.2 g of material, ground under liquid nitrogen, were used for spectrophotometric analysis of total anthocyanins according to Klopotek et al. (2005) expressing the values as µg of pelargonidin-3-glucoside/g fresh weight.

Statistical analyses

Depending on whether the data were normally distributed, either a one-way ANOVA with post-hoc Tukey test, or a Kruskal-Wallis statistical test with post-hoc Wilcoxon rank-sum was used to find statistical differences in gene expression between treatments. *P* values of <0.05 were considered significant.

RESULTS

To better understand the effects of chilled storage on strawberry fruit gene expression, genes associated with the H3K27me3 mark post-harvest were identified. Halved fruit, typically used in prepared fruit salads, were assessed at harvest and after 5 days storage at 8 °C. Seeds were removed to focus on the changes in the fleshy receptacle.

H3K27me3 profile changes during strawberry fruit storage

Prior to sequencing, the effectiveness of the H3K27me3 ChIP pull down was tested by real time qPCR for both DNA extracted from fruit at day 0 (at harvest) and day 5 (following 5 days of chilled dark storage) samples. Two genes were selected, based on their regulation by H3K27me3 in Arabidopsis (Zhang et al., 2007). Orthologous genes were identified in the *F. vesca* genome and ranked on sequence identity. To ensure the selected genes were expressed in the fruit, the strawberry eFP browser (Hawkins et al., 2017) was used to identify the top ten genes that had low expression in fruit at the red ripe stage and high expression in other tissues. The genes selected were: strawberry gene Fxa4Ag102286 which is annotated as WRKY75 and Fxa7Ag202455 which is annotated as LOB domain-containing protein. The ChIP-qPCR data showed successful pull-down of Fxa4Ag102286 and Fxa7Ag202455 with both being above 10% enriched in the H3K27me3 immunoprecipitation compared to the input at both time points (Supplementary Fig. S2A), while the control, 18S rRNA, was not enriched. The subsequent ChIP-seq and RNA-seq data confirmed that H3K27me3 peaks were associated with both these genes but there were very few RNA-seq reads, thus suggesting they have been silenced at both time points (Supplementary Fig. 2B)

Overall, between 46,036,568 and 77,704,802 reads were obtained for each sample from the ChIP-seq, comprising fruit from *Fragaria x ananassa* cv. Elsanta at harvest and after 5 days of chilled dark storage. On average, 31,570,868 for the H3K27me3 ChIP pull-down and 57,844,169 for the input

samples were mapped to the *Fragaria x ananassa* cv. Royal Royce genome. Reads were also mapped to two other available genomes *Fragaria x ananassa* cv. Camarosa and *Fragaria vesca* but the cv. Royal Royce provided the best % mapped reads (Supplementary Table S3). An inspection of the GC content revealed the presence of some bacterial DNA (Supplementary Fig. 3); these sequences are unlikely to have mapped onto the genome and therefore would not interfere with further analyses.

Principal component analysis grouped the pseudo-replicates by day of storage (Fig. 1A) and they showed good grouping in a correlation heatmap (Fig. 1B). The ChIP-seq peaks largely occurred within the promoter region and were less frequent in the gene body (5' UTRs, exons, introns, and 3'UTRs) (Fig. 1C). Some peaks occurred in the distal intergenic region: the genomic region located between two genes or gene loci but relatively distant from both. The peaks also seemed to decrease across the gene body, dropping just after the transcription start site (TSS) (Fig. 1D). The median peak length for day 0 was 1045 bp and 922 bp for day 5. The average peak length was 1966 bp for day 0 and 1783 bp for day 5.

A total of 45,753 H3K27me3 ChIP peaks were annotated across the two time points of strawberry fruit storage, with the majority shared between day 0 and day 5 (Fig 1E). However over 5,000 peaks (12.6%) were unique to day 0 and over 9,000 peaks (20%) were unique to day 5 fruit, indicating that the pattern of H3K27me3 binding changes during storage. The strawberry genome contains 101,793 protein coding genes (*Fragaria x ananassa* Royal Royce v1.0), thus in total day 0 peaks cover ~36% of the total gene number and day 5 covers ~39%.

Over 400 genes are potentially down-regulated by H3K27me3 modification

To assess whether H3K27me3 modifications might be correlated with gene expression during fruit storage the annotated H3K27me3 ChIP peaks were compared to differentially expressed genes (DEGs) from a transcriptomic analysis of the same fruit material. Over 75% of the RNA-seq reads mapped to the 'Royal Royce' reference genome (Supplementary Table S4) with an average of total of over 86 million reads for both day 0 and day 5. A total of 62,626 genes were expressed at day 0, and 63,840 genes at day 5 of storage. By HISAT2 analysis, 6,382 DEGs, (padj < 0.05, log2fold change

|>1) were identified between day 0 and day 5 of cold dark storage, with 2,292 down and 4,090 up-regulated (Supplementary Fig. S4A). GO annotation of all DEGs showed defence response as the most significantly changed biological process and extracellular region and cell wall as the most enriched components (Supplementary Fig. S4B). KEGG enrichment showed that phenylpropanoid biosynthesis was the most enriched metabolic pathway (Supplementary Fig. S4C). Other pathways that were significantly enriched include MAPK signalling, starch and sucrose metabolism, and flavonoid biosynthesis (Supplementary Table. S5).

A comparison of the annotated RNA-seq and ChIP-seq peaks (Supplementary Fig. S5) revealed 41,325 genes expressed at day 0, and 37,493 genes expressed at day 5 that were not associated with the H3K27me3 mark on each of those days. The majority of expressed genes at day 0 and day 5 were not associated with H3K27me3, as expected given the repressive role of H3K27me3. However, a further 21,301 genes on day 0, and 26,347 on day 5 were both expressed and associated with ChIP peaks. Of those ChIP peaks that were not associated with expressed genes at each timepoint, 11,744 were shared. GO term annotation of these repressed genes (Supplementary Table S6) is broadly consistent with functions expected to be repressed in fruit including flower and shoot system development, and several biosynthetic processes.

Comparison of RNA-seq DEGs and ChIP-seq peaks (Fig. 2A) included 131 genes that were up-regulated at day 5 compared to day 0 in the RNA-seq analysis and corresponded to ChIP-seq peaks at day 0 but not at day 5. Conversely, 309 genes which were down-regulated at day 5 were associated with ChIP-seq peaks at day 5 but not day 0 (Supplementary Table S7). The pattern of expression change and ChIP-seq peaks for these genes is consistent with a potential repression of their gene expression during storage by H3K27me3 binding. The position of the histone mark is also consistent with their regulation by H3K27me3: 203 were found within the promoter region (-2000 bp from TSS) and 362 were found within -2000 to +2000 bp to the TSS. However, a significant number of the DEGs were not associated with ChIP-seq peaks, and vice versa, and a further 2,529 DEGs (1,733 upregulated and 796 down-regulated) showed an unexpected positive correlation between ChIP-seq peaks and gene expression levels.

GO term enrichment showed that many of the 440 genes whose expression and ChIP peaks negatively correlate over storage, consistent with them being repressed by H3K27me3, were associated with temperature, cold, water deprivation and water (Fig 2B). The genes whose expression was up-regulated during storage were more represented in the enriched GO terms: “response to stress”, “response to abiotic stimulus” and responses to oxygen containing compounds and acids. The most significant term was “response to abiotic stimulus” and this was also the term that included the highest proportion of the down-regulated genes amongst the group of 440 genes.

Six GO terms were also shared between the whole RNA-seq data set and the 440 genes likely to be H3K27me3-regulated. Three of these: GO:0071944 - "cell periphery", GO:0016759 - "cellulose synthase activity", GO:0016760 - "cellulose synthase (UDP-forming) activity" relate to cell wall metabolism. Of the 50 genes in these GO terms the vast majority (41/50) were down regulated in expression during storage. The other GO terms represented were: GO:0016872 - "intramolecular lyase activity" GO:0030246 - "carbohydrate binding" and GO:0030001 - "metal ion transport".

H3K27me3-associated genes include transcription factors and metabolic genes

Seven of these H3K27me3-associated genes were selected for validation of their expression during fruit storage (Fig. 3A). Genes were selected to represent functions and processes associated with fruit storage: general stress responses, cold stress response, cell death, and fruit quality, identified in the RNA-seq KEGG and GO-enrichment analysis. The seven genes include two transcription factors (HY5 and TRAB1), one related to starch and sucrose metabolism (SS2), response to cold (ADH), flavonoid biosynthesis (CHI3), cell wall degradation (PL20), and cell death (FA2H). All seven genes were down regulated between day 0 and day 5 of storage in agreement with the RNA-seq data (Fig. 3B).

Of these, three were used to validate the ChIP-seq data: alcohol dehydrogenase like (Fxa2Ag101499), HY5 (Fxa2Ag102914) and TRAB1 (Fxa2Dg200568). ChIP-seq IGV tracks aligned to the RNA-seq tracks (Fig. 4A) show a ChIP peak close to the promoter region of each of the three genes at the transcriptional start site or just before it. ChIP-qPCR for these three genes showed the expected

repressive trend associated with H3K27me3 modification, with the day 5 sample being more enriched than the day 0 sample, although the difference was not significant perhaps due to the large variation between the biological replicates (Fig. 4B).

FaTRAB1 negatively regulates *FaMADS1* (Fxa6Cg103935) during fruit ripening (Lu et al., 2023). *FaMADS1* was up-regulated during fruit storage between day 0 and day 5 (Fig. 4C) although the change was not significant probably due to high variability in the day 0 expression across replicates. Downstream of TRAB1 and HY5 are genes related to the biosynthesis of anthocyanins (Lu et al., 2023; Liu et al., 2023b; Li et al., 2020). The effect of chilled postharvest storage at 8 °C in the dark on total anthocyanins was therefore compared to storage at 20 ˚C in the light (Fig. 4D). There was a significant increase in anthocyanin content when fruit were stored at 20 ˚C in the light whereas there was no significant increase when stored at 8 °C in the dark ($p < 0.05$).

DISCUSSION

An analysis of the chromatin profile of strawberry fruit during chilled post-harvest storage indicated that there was an association between several thousand genes expressed during postharvest storage and the H3K27me3 mark.

The position of the H3K27me3 peaks relative to the gene differs to that seen in other plant systems such as peach buds (de la Fuente et al., 2015), Arabidopsis seedlings (Zhang et al., 2007) and *Brassica rapa* leaves and inflorescences (Payá-Milans et al., 2019) where the peaks are distributed evenly across the gene body. Here we detected a bias toward the 5’ end of the gene with peaks concentrated largely within the first 1000 bp of the promoter around the TSS, decreasing across the gene body towards the 3’ end. This unusual distribution of the H3K27me3 mark is in agreement with its distribution on two expansin genes previously described in *F. vesca* (Mu et al., 2021), suggesting a non-canonical distribution of H3K27me3 marks on strawberry chromatin. The H3K27me3 pattern observed here does not appear to be related to the tissue type as the more canonical distribution of H3K27me3 has been described for another soft fruit, tomato (Cigliano et al., 2022). Nor does this

pattern appear to be a feature of the *Rosaceae* in general since in peach buds the H3K27me3 distribution was as expected (de la Fuente et al., 2015). Indeed, the H3K27me3 pattern in strawberry is more reminiscent of the distribution of the H3K4me3 mark, a chromatin modification generally associated with a positive regulation of gene expression (Foroozani et al., 2021). The median length of the H3K27me3 marked regions (987 bp) was more similar to that found in peach buds and Arabidopsis seedlings (de la Fuente et al., 2015; Zhang et al., 2007) while in the *B. rapa* study (Payá-Milans et al., 2019) the marked region was over 2 kb. This indicates that the H3K27me3 deposition mechanism may be different in strawberry fruit compared to other plant species and tissues.

The 39% of genes associated with H3K27me3 modification (and 12% of the genome) found here in chilled stored mature strawberry fruit is high compared to some other studies with ~27% in *Brassica rapa* leaves and inflorescences ~17% in Arabidopsis seedlings (Payá-Milans et al., 2019; Zhang et al., 2007) and 6.2% of the genome in tomatoes stored at room temperature (Cigliano et al., 2022). However, H3K27me3 is detected on as many as 60% of protein-coding genes in the Arabidopsis shoot apical meristem (You et al., 2017) indicating that the proportion of silenced genes can vary widely across species and tissues. The H3K27me3 has not to date been assessed for its role in regulating genes in mature strawberry fruit, hence a high number of H3K27me3 is possible in this highly differentiated tissue. Given the repressive nature of the H3K27me3 mark this would suggest that it is involved in wide scale repression of gene expression in mature strawberry fruit.

Although 440 genes were identified whose expression pattern is consistent with H3K27me3 mediated gene repression, a large number of the H3K27me3 associated genes did not show this pattern. Indeed over 20,000 genes at each timepoint were expressed but associated with the repressive H3K27me3 mark. Note that for example bivalent domains have been discovered where chromatin is modified both in an active and repressive way simultaneously (Bernstein et al., 2006; Faivre and Schubert, 2023). Indeed, H3K27me3 does not always prevent gene transcription and the independent accumulation of the active H3K4me3 mark (Liu et al., 2014). For example, in potato cold stress increased chromatin accessibility at bivalently H3K4me3 and H3K27me3 marked active genes (Zeng et al., 2019).

The presence of bacterial DNA in the ChIP-seq dataset is consistent with an increase in microflora development over the 5 days of storage noted in other post-harvest studies (e.g. Wang et al., 2018). Of the 440 genes whose expression pattern is consistent with repression by H3K27me3, 16 were annotated as responding to biotic stimuli. This raises the possibility that H3K27me3 may be regulating responses to the increase in microflora associated with post-harvest storage.

The number of ChIP peaks increased at day 5 of storage compared to day 0 indicating that the role of this repressive mark is increasing. In comparison a post-harvest study in tomato showed a reduction of genes associated with the H3K27me3 mark during storage (Cigliano et al., 2022) and it was suggested that H3K27me3 loss could be responsible for activating genes required for fruit softening and senescence. However, in Cigliano et al. (2022) the fruit was not chilled during storage suggesting that the increase in H3K27me3 associated genes may be influenced by the storage conditions.

GO term enrichment indicated that the most significant group of H3K27me3-regulated genes whose expression changes during storage are involved in abiotic stress responses, and the majority of these are down-regulated. This is perhaps unexpected given that cold storage is likely imposing abiotic stress. Down-regulation of abiotic stress-responsive genes was previously recorded for halved strawberries between day 1 and 5 of storage at 8 $^{\circ}$C (Baldwin et al., 2023) and maybe due to effects of post-harvest senescence on the ability of the fruit to respond to the stress.

GO term enrichment also suggested that cold stress genes may be regulated by H3K27me3 in the stored fruit, although again expression of the majority of these genes was down-regulated with fruit storage. This contrasts with a fall in the H3K27me3 mark associated with the activation of stress-responsive transcription factors in cold stressed rice seedlings (Dasgupta et al., 2022). In Arabidopsis seedlings, cold stress caused a permanent decrease of H3K27me3 association in some cold responsive genes (Kwon et al., 2009). Thus, association to H3K27me3 is cold sensitive, and may cause permanent alterations in the epigenetic state. However, here the effect of cold storage seems to increase gene repression via H3K27me3 rather than alleviate it.

The integration of RNA-seq and ChIP-seq data also suggested a role for H3K27me3 in the regulation of cell wall breakdown. This is consistent with the loss H3K27me3 modification associated with *FveEXP33* expression during *Fragaria vesca* fruit ripening (Mu et al., 2021) as EXP proteins participate in cell wall loosening and therefore play a role in fruit ripening and softening (Moya-Leon et al., 2019). Here, a close match to *FveEXP33*, Fxa7Bg202431, was included in the 440 genes likely to be H3K27me3-regulated, but was down-regulated during fruit storage. Indeed, the majority of the cell wall associated genes here associated with H3K27me3 changes were down-regulated, suggesting that during storage there is a repression of cell wall modulation, perhaps as a result of a cold-induced lowering of the metabolic rate.

Strawberry fruit are non-climacteric (Gu et al., 2019) and ripening after harvest is limited, but does include increases in anthocyanins (Chen et al., 2014). Chilled storage delays the post-harvest ripening process in strawberries and is used in the supply chain to maintain quality. It was shown here to abolish the rise in anthocyanins seen during post-harvest ripening at ambient temperature. One of the genes used to validate the ChIP-seq, *FaHY5* (Fxa2Ag102914) is light-induced, and in *F. vesca FvHy5* regulates anthocyanin biosynthesis (Liu et al., 2023b) via a complex with FvbHLH9. Moreover, in *F. ananassa* a B-box transcription factor, FaBBX22, interacts with FaHY5 to promote anthocyanin accumulation in strawberry fruits (Liu et al., 2022). The finding here that *FaHY5* is repressed during fruit storage and is associated with the H3K27me3 mark provides a further potential mechanism for the regulation of anthocyanin biosynthesis in strawberry fruit. Its repression may be part of the shutting down of fruit ripening by the combination of the cold and dark storage conditions generally used in the supply chain and applied here.

The confirmation of ADH as another gene repressed during fruit storage, and its association with the H3K27me3 mark during storage of strawberry fruit is of interest as ADH is a key enzyme in ester biosynthesis, and esters are major components of strawberry aroma (Yan et al., 2018). Chilled storage has significant effects on volatile organic compound profile of strawberries (Baldwin et al., 2023) including a reduction in the relative abundance of esters, especially non-acetate esters. The final enzyme in ester biosynthesis alcohol acyltransferase (AAT) was also down-regulated during

strawberry fruit storage (Baldwin et al., 2023) but was not associated with a H3K27me3 ChIP-seq peak, indicating that different mechanisms operate to modulate different steps of ester biosynthesis during fruit storage.

FaTRAB1 is also an important gene in strawberry fruit ripening and aroma development, as it represses the expression of *FaMADS1* through an ABA-dependent mechanism (Lu et al., 2023). In turn FaMADS1 represses a number of ripening-related genes including AAT. The H3K27me3 dependent down-regulation of *FaTRAB1* during cold storage would therefore be expected to up-regulate *FaMADS1* expression which indeed it does. The role of these genes can be summarised in a model (Fig. 5). The model predicts that during dark chilled storage, HY5, TRAB1 and ADH expression is subject to H3K27me3 dependent down-regulation. This leads to a reduction of anthocyanin and ester biosynthesis through two linked routes. Repression of the activator HY5 and the de-repression of the repressor MADS1 results in the reduction of anthocyanin biosynthesis, and de-repression of MADS1 and repression of ADH results in the reduction of ester formation. Our model is supported by (i) a lack of anthocyanin accumulation and a reduction in ester production during chilled dark storage, (ii) the association of H3K27me3 marks with HY5, TRAB1 and ADH during chilled dark storage, and (iii) the reduced expression of HY5, TRAB1 and ADH and increased expression of MADS1 during chilled dark storage.

In conclusion, the exploration of the effects of H3K27me3 regulation on gene expression during strawberry fruit storage reveals mechanisms for the repression of key genes associated with strawberry ripening. This provides additional mechanisms for regulating aroma production post-harvest and potential targets for improving aroma retention in the supply chain.

Acknowledgements

We thank the School of Biosciences, Cardiff University Genomics Research Technology Hubs for their assistance with the ChIP-seq sequence analysis, with a particular thanks to Angela Marchbank for assistance in sequencing advice.

Author contributions

Investigation and Methodology: AB, KL, RAL, RJH, AM, CLW; Formal Analysis: AB and TL; Conceptualisation, Project Administration Supervision and Funding acquisition: AB, HJR,SS and H-W N. Writing: Draft, Review and Editing: AB, TL, AM, SS, KL, CLW, RAL, RJH, H-WN, HJR.

Conflict of interest

No conflict of interest declared.

Funding

AB was funded by the BBSRC through the SWBio DTP programme and with support from Edward Vinson Ltd.

Data availability

Sequencing data are deposited in the NCBI Sequence Read Archive (http://www.ncbi.nlm.nih.gov/Traces/sra) under BioProject ID. PRJNA1096352.

References

Baldwin A, Dhorajiwala R, Roberts C, et al. 2023. Storage of halved strawberry fruits affects aroma, phytochemical content and gene expression, and is affected by pre-harvest factors. Frontiers in Plant Science **14,** 1165056..

Bernstein BE, Mikkelsen TS, Xie X, et al. 2006. A Bivalent chromatin structure marks key developmental genes in embryonic stem cells. Cell **125,** 315-326.

Cao X, Wei C, Duan W, Gao Y, Kuang J, Liu M, Chen K, Klee H, Zhang B. 2021. Transcriptional and epigenetic analysis reveals that NAC transcription factors regulate fruit flavor ester biosynthesis. The Plant Journal **106**, 785–800.

Carroll TS, Liang Z, Salama R, Stark R, de Santiago I. 2014. Impact of artifact removal on ChIP quality metrics in ChIP-seq and ChIP-exo data. Frontiers in Genetics **5**, 75.

Chen J, Mao L, Mi H, Zhao Y, Ying T, Luo Z. 2014. Detachment-accelerated ripening and senescence of strawberry (*Fragaria* × *ananassa* Duch. *cv.* Akihime) fruit and the regulation role of multiple phytohormones. Acta Physiologiae Plantarum **36,** 2441-2451.

Chen J, Mao L, Mi H, Lu W, Ying T, Luo Z. 2016. Involvement of abscisic acid in postharvest water-deficit stress associated with the accumulation of anthocyanins in strawberry fruit. Postharvest Biology and Technology, **111**, 99-105.

Chen S, Zhou Y, Chen Y, Gu J. 2018. Fastp: An ultra-fast all-in-one FASTQ preprocessor. Bioinformatics **34,** i884–i890.

Cigliano RA, Aversano R, Di Matteo A, et al. 2022. Multi-omics data integration provides insights into the post-harvest biology of a long shelf-life tomato landrace. Horticulture Research **9,** uhab042.

Dasgupta P, Prasad P, Bag SK, Chaudhuri S. 2022. Dynamicity of histone H3K27ac and H3K27me3 modifications regulate the cold-responsive gene expression in *Oryza sativa* L. ssp. indica. Genomics **114,** 110433.

de la Fuente L, Conesa A, Lloret A, Badenes ML, Ríos G. 2015. Genome-wide changes in histone H3 lysine 27 trimethylation associated with bud dormancy release in peach. Tree Genetics and Genomes **11,** 1-14.

Dhorajiwala R, Roberts C, Dimitrova S, et al. 2021. Storage of halved strawberry fruits affects aroma, phytochemical content and gene expression. Acta Horticulturae, **1309**, 887–896..

Edger PP, Poorten TJ, VanBuren R, et al. 2019. Origin and evolution of the octoploid strawberry genome. Nature Genetics **51,** 541–547.

Ewels P, Magnusson M, Lundin S, Käller M. 2016. MultiQC: Summarize analysis results for multiple tools and samples in a single report. Bioinformatics **32**, 3047-3048.

Faivre L, Schubert D. 2023. Facilitating transcriptional transitions: an overview of chromatin bivalency in plants. Journal of Experimental Botany **74**, 1770-1783.

Feliziani E, Romanazzi G. 2016. Postharvest decay of strawberry fruit: Etiology, epidemiology, and disease management. Journal of Berry Research, **6**, 47-63.

Foroozani M, Vandal MP, Smith AP. 2021. H3K4 trimethylation dynamics impact diverse developmental and environmental responses in plants. Planta **253**, 1-7.

Greco M, Sáez CA, Brown MT, Bitonti MB. 2014. A simple and effective method for high quality co-extraction of genomic DNA and total RNA from low biomass *Ectocarpus siliculosus*, the model brown alga. PLoS ONE **9**, e96470.

Gu T, Ren S, Wang Y, Han Y, Li Y. 2016. Characterization of DNA methyltransferase and demethylase genes in Fragaria vesca. Molecular Genetics and Genomics **291,** 1333-1345.

Gu T, Jia S, Huang X, Wang L, Fu W, Huo G, Gan L, Ding J, Yi, L. 2019. Transcriptome and hormone analyses provide insights into hormonal regulation in strawberry ripening. Planta **1**, 145–162.

Hardigan MA, Feldmann MJ, Pincot DDA, et al. 2021. Blueprint for Phasing and Assembling the Genomes of Heterozygous Polyploids: Application to the Octoploid Genome of Strawberry. bioRxiv, 2021.11.03.467115.

Hawkins C, Caruana J, Li J, Zawora C, Darwish O, Wu J, Alkharouf N, Liu Z. 2017. An eFP browser for visualizing strawberry fruit and flower transcriptomes. Horticulture Research **4,** 17029.

Huang X, Pan Q, Lin Y, Gu T, Li Y. 2020. A native chromatin immunoprecipitation (ChIP) protocol for studying histone modifications in strawberry fruits. Plant Methods **16**, 1–12.

Jia HF, Chai YM, Li CL, Lu D, Luo JJ, Qin L, Shen YY. 2011. Abscisic acid plays an important role in the regulation of strawberry fruit ripening. Plant Physiology **157,** 188-199.

Kim SK, Bae RN, Na H, Dal Ko K, Chun C. 2013. Changes in physicochemical characteristics during fruit development in June-bearing strawberry cultivars. Horticulture, Environment, and Biotechnology, **54**, 44-51

Kim D, Paggi JM, Park C, Bennett C, Salzberg SL. 2019. Graph-based genome alignment and genotyping with HISAT2 and HISAT-genotype. Nature Biotechnology, **37**, 907-915.

Klopotek Y, Otto K, Böhm V. 2005. Processing strawberries to different products alters contents of vitamin C, total phenolics, total anthocyanins, and antioxidant capacity. Journal of Agricultural and Food Chemistry, **53**, 5640-5646.

Kwon CS, Lee D, Choi G, Chung W I. 2009. Histone occupancy-dependent and -independent removal of H3K27 trimethylation at cold-responsive genes in Arabidopsis. Plant Journal **60**, 112-121.

Langmead B, Salzberg S L 2012. Fast gapped-read alignment with Bowtie 2. Nature Methods, **9**, 357-359.

Li Z, Wang Z, Wang K, Liu Y, Hong Y, Chen C, Guan X, Chen Q. 2020. Co-expression network analysis uncovers key candidate genes related to the regulation of volatile esters accumulation in woodland strawberry. Planta, 252, 1-15.

Li X, Martín-Pizarro C, Zhou L, Hou B, Wang Y, Shen Y, Li B, Posé D, Qin G. 2023. Deciphering the regulatory network of the NAC transcription factor FvRIF, a key regulator of strawberry (*Fragaria vesca*) fruit ripening. The Plant Cell **35,** 4020-4045.

Liu C, Lu F, Cui X, Cao X. 2010. Histone methylation in higher plants. Annual Review of Plant Biology **61,** 395-420.

Liu Y, Ye Y, Wang Y, Jiang L, Yue M, Tang L, Jin M, Zhang Y, Lin Y, Tang H. 2022. B-Box transcription factor FaBBX22 promotes light-induced anthocyanin accumulation in strawberry (*Fragaria* × *ananassa*). International Journal of Molecular Sciences **23**, 7757.

Liu N, Fromm M, Avramova Z. 2014. H3K27me3 and H3K4me3 chromatin environment at super-induced dehydration stress memory genes of *Arabidopsis thaliana*. Molecular Plant **7**, 502-513..

Liu G. Huang L. Lian J. 2023. Alcohol acyltransferases for the biosynthesis of esters. Biotechnology for Biofuels and Bioproducts, **16**, 93.

Liu Y, Tang L, Wang Y,et al. (2023b). The blue light signal transduction module FaCRY1-FaCOP1-FaHY5 regulates anthocyanin accumulation in cultivated strawberry. Frontiers in Plant Science, **14**, 1144273.

Livak KJ, Schmittgen TD. 2001. Analysis of relative gene expression data using real-time quantitative PCR and the 2-ΔΔCT method. Methods **25**, 402–408.

Love M I, Huber W, Anders S. 2014. Moderated estimation of fold change and dispersion for RNA-seq data with DESeq2. Genome Biology 15, 550.

Lu W, Wei X, Han X, Chen R, Xiao C, Zheng X, Mao L. 2023. Participation of FaTRAB1 transcription factor in the regulation of *FaMADS1* involved in ABA-dependent ripening of strawberry fruit. Foods **12**, 1802.

Medina-Puche L, Cumplido-Laso G, Amil-Ruiz F, Hoffmann T, Ring L, Rodríguez-Franco A, Caballero JL, Schwab W, Muñoz-Blanco J, Blanco-Portales R. 2014. *MYB10* plays a major role in

the regulation of flavonoid/phenylpropanoid metabolism during ripening of *Fragaria* × *ananassa* fruits. Journal of Experimental Botany **65**, 401-417.

Moya-León MA, Mattus-Araya E, Herrera R. 2019. Molecular events occurring during softening of strawberry fruit. Frontiers in Plant Science **10**, 615.

Mu Q, Li X, Luo J, Pan Q, Li Y, Gu T. 2021. Characterization of expansin genes and their transcriptional regulation by histone modifications in strawberry. Planta **254**, 1-14.

Nakato R, Sakata T. 2021. Methods for ChIP-seq analysis: A practical workflow and advanced applications. Methods **187**, 44–53.

Payá-Milans M, Poza-Viejo L, Martín-Uriz PS, Lara-Astiaso D, Wilkinson MD, Crevillén P. 2019. Genome-wide analysis of the H3K27me3 epigenome and transcriptome in *Brassica rapa*. GigaScience **8**, 1–13.

Petrasch S, Mesquida-Pesci SD, Pincot DDA, Feldmann MJ, López CM, Famula R, Hardigan MA, Cole GS, Knapp SJ, Blanco-Ulate B. 2022. Genomic prediction of strawberry resistance to postharvest fruit decay caused by the fungal pathogen *Botrytis cinerea*. G3: Genes, Genomes, Genetics **12**, jkab378. .

Quinlan AR, Hall IM. 2010. BEDTools: A flexible suite of utilities for comparing genomic features. Bioinformatics **26**,.841-842.

Romanazzi G, Smilanick JL, Feliziani E, Droby S. 2016. Integrated management of postharvest gray mold on fruit crops. Postharvest Biology and Technology. **113**, 69-76.

Rozen S, Skaletsky H. 2000. Primer3 on the WWW for general users and for biologist programmers. Bioinformatics Methods and Protocols **132**, 365–386.

Sánchez-Gómez C, Posé D, Martín-Pizarro C. 2022. Insights into transcription factors controlling strawberry fruit development and ripening. Frontiers in Plant Science, **13**, 1022369.

Siebeneichler TJ, Crizel RL, Camozatto GH, Paim BT, da Silva Messias R, Rombaldi CV, Galli V. 2020. The postharvest ripening of strawberry fruits induced by abscisic acid and sucrose differs from their in vivo ripening. Food Chemistry **317**, 126407.

Stark R, Brown G. 2011. DiffBind: differential binding analysis of ChIP-Seq peak data. Available online at: http://bioconductor.org/packages/release/bioc/html/DiffBind.html.

Tennessen JA, Govindarajulu R, Ashman TL, Liston A. 2014. Evolutionary origins and dynamics of octoploid strawberry subgenomes revealed by dense targeted capture linkage maps. Genome Biology and Evolution **6**, 3295-3313.

Tian F, Yang DC, Meng YQ, Jin J, Gao G. 2020. PlantRegMap: charting functional regulatory maps in plants. Nucleic Acids Research **48**, D1104–D1113.

Voća S, Dobričević N, Skendrović Babojelić M, Družić J, Duralija B, Levačić J. 2007. Differences in fruit quality of strawberry cv. Elsanta depending on cultivation system and harvest time. Agriculturae Conspectus Scientificus **72**, 285-288.

Walter W, Sánchez-Cabo F, Ricote M. 2015. GOplot: An R package for visually combining expression data with functional analysis. Bioinformatics **31**, 2912-2914.

Wang W, Hu W, Ding T, Ye X, Liu D. 2018. Shelf- life prediction of strawberry at different temperatures during storage using kinetic analysis and model development. Journal of Food Processing and preservation, **42**, e13693.

Yan JW, Ban ZJ, Lu HY, Li D, Poverenov E, Luo ZS, Li L. 2018. The aroma volatile repertoire in strawberry fruit: A review. Journal of the Science of Food and Agriculture. **98**, 4395-402.

Yang Z, Cao S, Su X, Jiang Y. 2014. Respiratory activity and mitochondrial membrane associated with fruit senescence in postharvest peaches in response to UV-C treatment. Food Chemistry **161**, 16–21.

You Y, Sawikowska A, Neumann M, Posé D, Capovilla G, Langenecker T, Neher RA, Krajewski P, Schmid M. 2017. Temporal dynamics of gene expression and histone marks at the Arabidopsis shoot meristem during flowering. Nature Communications **8**, 1–12.

Yu G, Wang LG, He QY. 2015. ChIP seeker: An R/Bioconductor package for ChIP peak annotation, comparison and visualization. Bioinformatics **31**, 2382-2383.

Yuan L, Wang D, Cao L, Yu N, Liu K, Guo Y, Gan S, Chen L. 2020. Regulation of leaf longevity by DML3-mediated DNA demethylation. Molecular Plant. **13**, 1149-61.

Yun Z, Jin S, Ding Y, Wang Z, Gao H, Pan Z, Xu J, Cheng Y, Deng X. 2012. Comparative transcriptomics and proteomics analysis of citrus fruit, to improve understanding of the effect of low temperature on maintaining fruit quality during lengthy post-harvest storage. Journal of Experimental Botany **63**, 2873–2893.

Zeng Z, Zhang W, Marand AP, Zhu B, Buell CR, Jiang J. 2019. Cold stress induces enhanced chromatin accessibility and bivalent histone modifications H3K4me3 and H3K27me3 of active genes in potato. Genome Biology **20**, 1–17.

Zhang X, Clarenz O, Cokus S, Bernatavichute Y V, Pellegrini M, Goodrich J, Jacobsen SE. 2007. Whole-genome analysis of histone H3 lysine 27 trimethylation in Arabidopsis. PLoS Biology **5**, e129.

Zhang Y, Liu T, Meyer CA, et al. 2008. Model-based analysis of ChIP-Seq (MACS). Genome Biology **9**, 1-9.

Zhang B, Tieman DM, Jiao C, Xu Y, Chen K, Fe Z, Giovannoni JJ, Klee HJ. 2016. Chilling-induced tomato flavor loss is associated with altered volatile synthesis and transient changes in DNA methylation. Proceedings of the National Academy of Sciences of the United States of America **113**, 12580–12585.

Zhang Y, Li Y, Zhang Y, Zhang Z, Zhang D, Wang X, Lai B, Huang D, Gu L, Xie Y, Miao Y. 2022. Genome-wide H3K9 acetylation level increases with age-dependent senescence of flag leaf in rice. Journal of Experimental Botany. **73**, 4696-715.

Figure Legends

Figure 1. ChIP-seq analysis of H3K27me3 profile across the *Fragaria* x *ananassa* genome comparing fruit at day 0 and day 5 of chilled dark storage **(A)** PCA plot showing pseudo-replicate grouping by day of storage using all read counts, **(B)** correlation heatmap, using H3K27me3 occupancy (peak caller score) data **(C)** Genomic annotation of H3K27me3 for day 0 and day 5. Bar charts show % of mapped peaks that were located in each genomic region. Promoter regions are divided into different portions; kb in brackets are distances from the TSS. **(D)** Profile of H3K27me3 ChIP peak frequency across gene body regions (TSS, transcription start site; TTS transcriptional termination site). Mean profiles of ChIP peaks are shown from each time point showing their location on the gene and the peak count frequency for that location; **(E)** Overlap between the annotated ChIP peaks from day 0 and day 5 stored strawberry fruit.

Figure 2. Comparison of H3K27me3 ChIP-seq and RNAseq datasets for stored strawberry fruit **(A)** Overlap in expression patterns of RNAseq DEGs (up and down regulated) and ChIP-seq peaks at day 0 and day 5 of chilled storage **(B)** GO term plot of the most significant GO terms (BP) in the 440 genes whose expression change between day 0 and day 5 of storage is consistent with H3K27me3 regulation. The outer circle shows a scatter plot for each term of the log2FC of the assigned genes. Red circles display up- regulation and blue ones down- regulation. The inner circle shows the significance of the GO term with a taller segment representing higher significance. Inner circle colour represents the GO term Z-score. This reports the proportion of up (increasing) and down (decreasing) regulated genes over storage represented in the GO term, compared to the set of 440 genes.

Figure 3. Seven genes from the ChIP-seq analysis selected for validation **(A)** *Fragaria x ananassa* Royal Royce code, closest matched *Fragaria vesca* code, % identity between the two sequences, Log 2-fold change from the RNA-seq analysis, annotated function, gene

name and associated GO/KEGG terms **(B)** Real time qPCR analysis of the expression of these genes (mean ± SD) in fruit at day 0 and day 5 of chilled storage (n=3). Asterisks are based on a t-test; ** P < 0.01; * P <0.05; ns, non-significant.

Figure 4. Validation of ChIP-seq data. **(A)** IGV tracks of RNA-seq data and ChIP-seq data. Red boxes highlight the gene, and the peak associated with it. The point of the red arrow shows the position of the TSS, arrow direction indicates orientation of the gene. **(B)** ChIP-qPCR data for *FaADH*, *FaHY5* and *FaTRAB1* showing % input over the two time points (mean ± SD, n=3) **(C)** Expression of FaMADS1 during fruit storage; real time qPCR and RNAseq Log2 FC in red (mean ± SD, n=3). **(D)** Total anthocyanin content of strawberries at harvest (H), and following storage for 5 days at 20 ºC or 8 ºC for 5 days (mean + SD, n=3, different letters indicate significant differences ($p<0.05$) based on a Dunn test.

Figure 5. Model showing H3K27me3 regulation of fruit metabolism during storage. Cold dark storage of ripe strawberry fruit results in repression of *FaHY5* transcription through the H3K27me3 mark. This reduces anthocyanin accumulation. Storage also represses FaTRAB1 through the H3K27me3 mark resulting in increased FaMADS1 expression which allows it to repress anthocyanin biosynthesis as well. An increase in MADS1 expression also represses AAT resulting in reduced ester production. ADH is also regulated by the H3K27me3 mark during storage resulting in reduced substrate for AAT, thus also contributing to repression of aroma development.

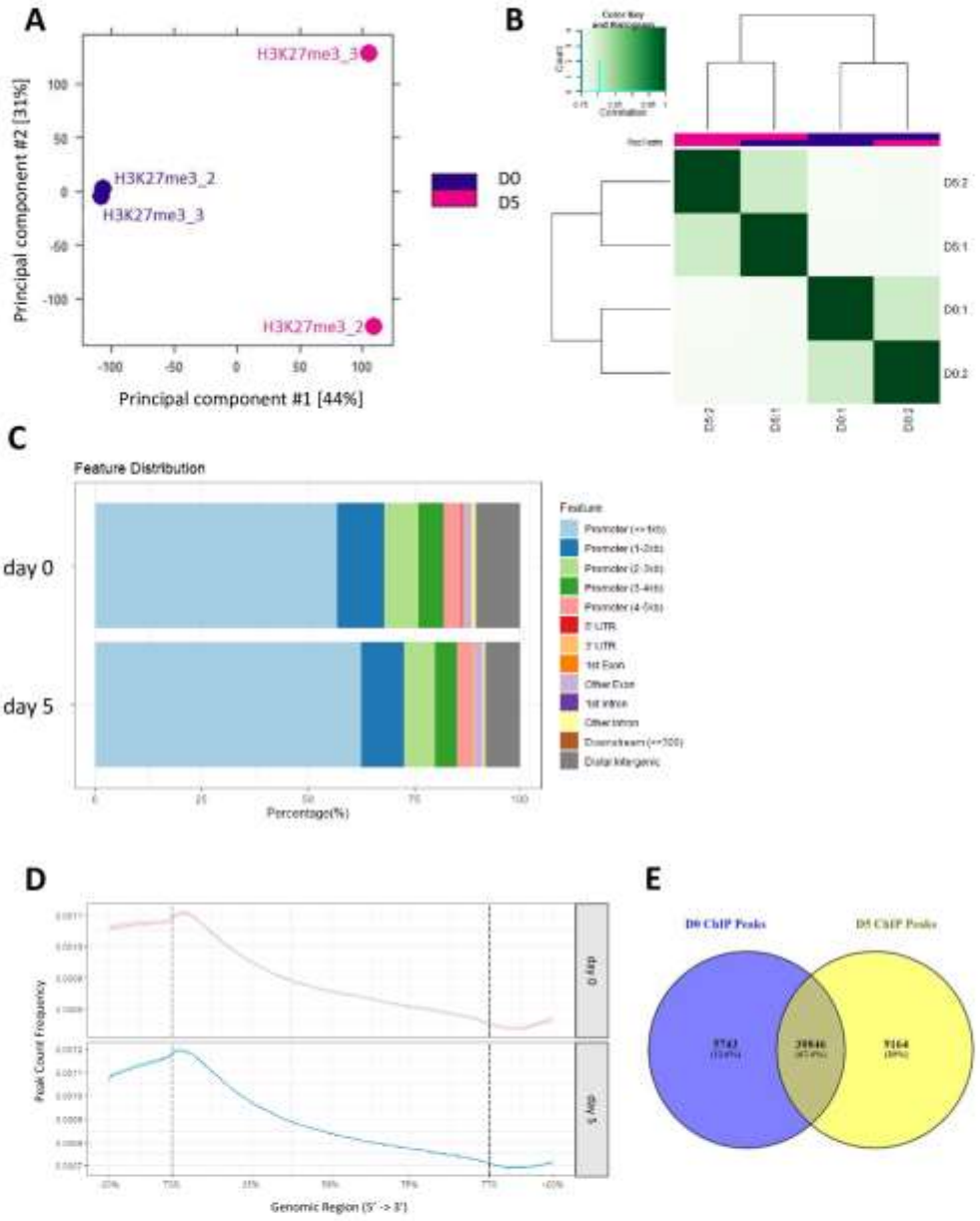

Figure 1. ChIP-seq analysis of H3K27me3 profile across the *Fragaria* x *ananassa* genome comparing fruit at day 0 and day 5 of chilled dark storage **(A)** PCA plot showing pseudo-replicate grouping by day of storage using all read counts, **(B)** correlation heatmap, using H3K27me3 occupancy (peak caller score) data **(C)** Genomic annotation of H3K27me3 for day 0 and day 5. Bar charts show % of mapped peaks that were located in each genomic region. Promoter regions are divided into different portions; kb in brackets are distances from the TSS. **(D)** Profile of H3K27me3 ChIP peak frequency across gene body regions (TSS, transcription start site; TTS transcriptional termination site). Mean profiles of ChIP peaks are shown from each time point showing their location on the gene and the peak count frequency for that location; **(E)** Overlap between the annotated ChIP peaks from day 0 and day 5 stored strawberry fruit.

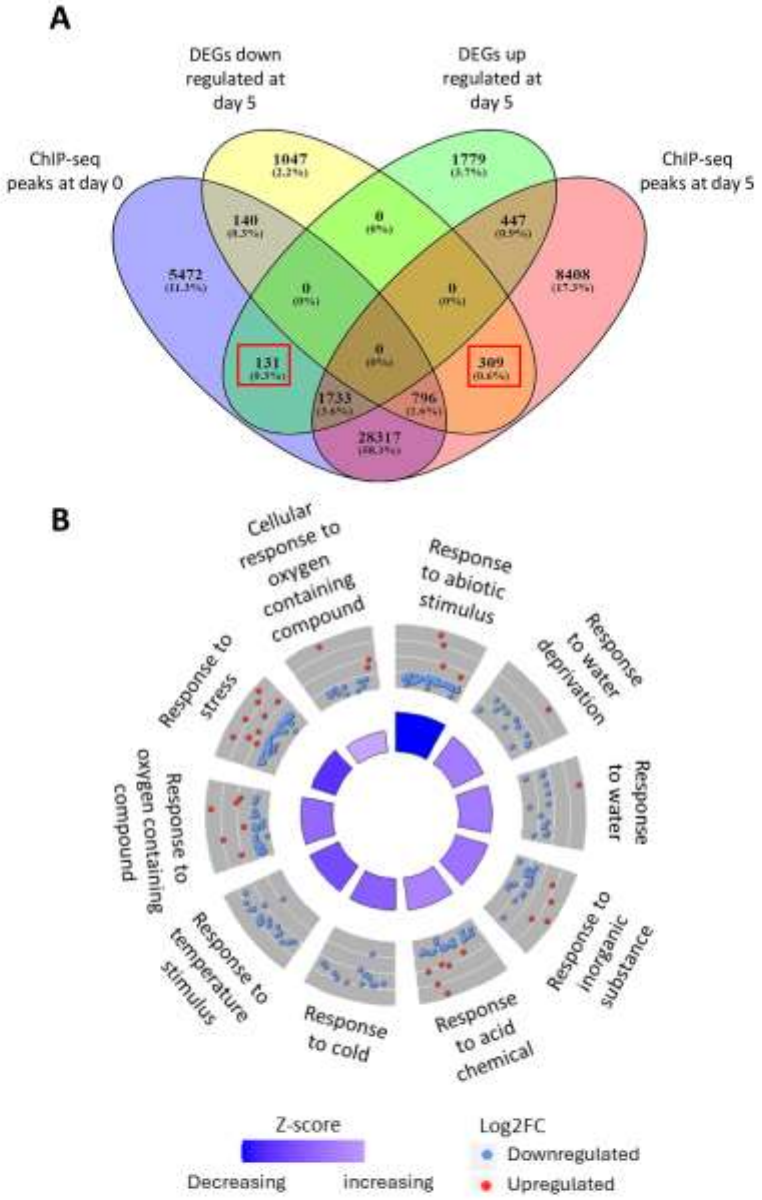

Figure 2. Comparison of H3K27me3 ChIP-seq and RNAseq datasets for stored strawberry fruit (A) Overlap in expression patterns of RNAseq DEGs (up and down regulated) and ChIP-seq peaks at day 0 and day 5 of chilled storage **(B)** GO term plot of the most significant GO terms (BP) in the 440 genes whose expression change between day 0 and day 5 of storage is consistent with H3K27me3 regulation. The outer circle shows a scatter plot for each term of the log2FC of the assigned genes. Red circles display up-regulation and blue ones down- regulation. The inner circle shows the significance of the GO term with a taller segment representing higher significance. Inner circle colour represents the GO term Z-score. This reports the proportion of up (increasing) and down (decreasing) regulated genes over storage represented in the GO term, compared to the set of 440 genes.

A

Fa RR gene code	Fv gene code	%ID Fa vs Fv	L2FC	Description	Gene name	Relevant GO/KEGG terms
Fxa2Ag102914	gene11666	98.05	-2.05	TF HY5	HY5	TF, response to hormone
Fxa7Dg102232	gene21346	97.21	-1.47	Probable chalcone--flavonone isomerase 3	CHI3	Response to abiotic stimulus
Fxa2Dg200568	gene28250	97.81	-1.34	bZIP TF TRAB1	TRAB1	TF, response to stress
Fxa2Ag101499	gene30068	99.73	-1.61	Alcohol dehydrogenase-like	ADH	Response to cold
Fxa6Ag104600	gene04452	99.61	-1.41	Granule-bound starch synthase 2	SS2	Starch and sucrose metabolism
Fxa2Bg201844	gene17555	98.47	-1.60	Probable pectate lyase 20	PL20	Cell wall degradation
Fxa3Ag101008	gene20188	92.50	-1.26	Fatty acid 2-hydroxylase 1-like	FA2H	Programmed cell death

B

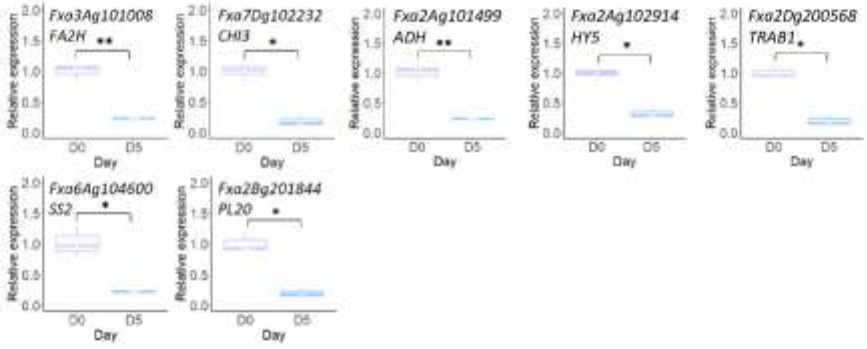

Figure 3. Seven genes from the ChIP-seq analysis selected for validation (A) *Fragaria x ananassa* Royal Royce code, closest matched *Fragaria vesca* code, % identity between the two sequences, Log 2-fold change from the RNA-seq analysis, annotated function, gene name and associated GO/KEGG terms **(B)** real time qPCR analysis of the expression of these genes (mean ± SD) in fruit at day 0 and day 5 of chilled storage (n=3). Asterisks are based on a t-test; ** $P < 0.01$; * $P < 0.05$; ns, non-significant.

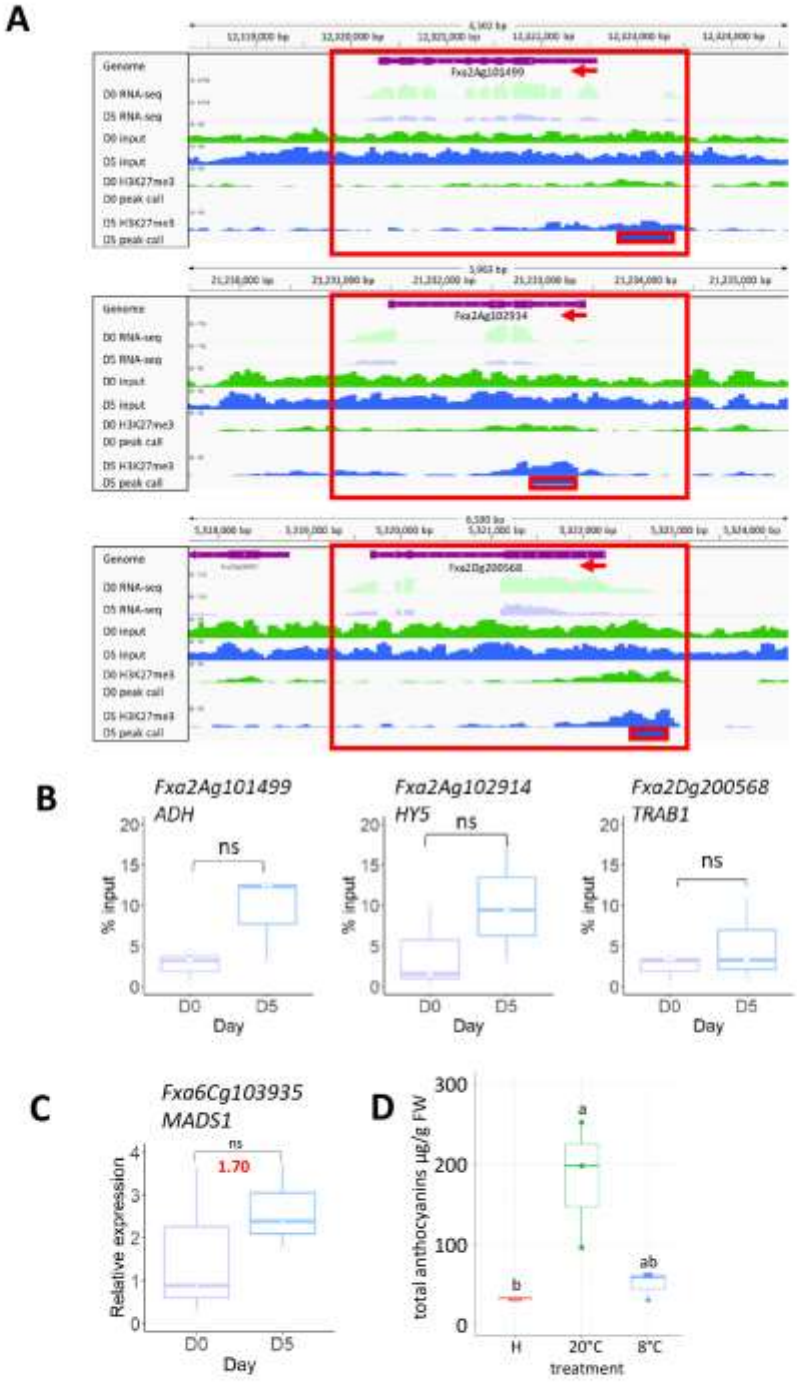

Figure 4. Validation of ChIP-seq data. **(A)** IGV tracks of RNA-seq data and ChIP-seq data. Red boxes highlight the gene, and the peak associated with it. The point of the red arrow shows the position of the TSS, arrow direction indicates orientation of the gene. **(B)** ChIP-qPCR data for *FaADH, FaHY5* and *FaTRAB1* showing % input over the two time points (mean ± SD, n=3) **(C)** expression of FaMADS1 during fruit storage; real time qPCR and RNAseq Log2 FC in red (mean ± SD, n=3); **(D)** Total anthocyanin content of strawberries at harvest (H), and following storage for 5 days at 20 ºC or 8 ºC for 5 days (mean ± SD, n=3, different letters indicate significant differences ($p<0.05$) based on a Dunn test.

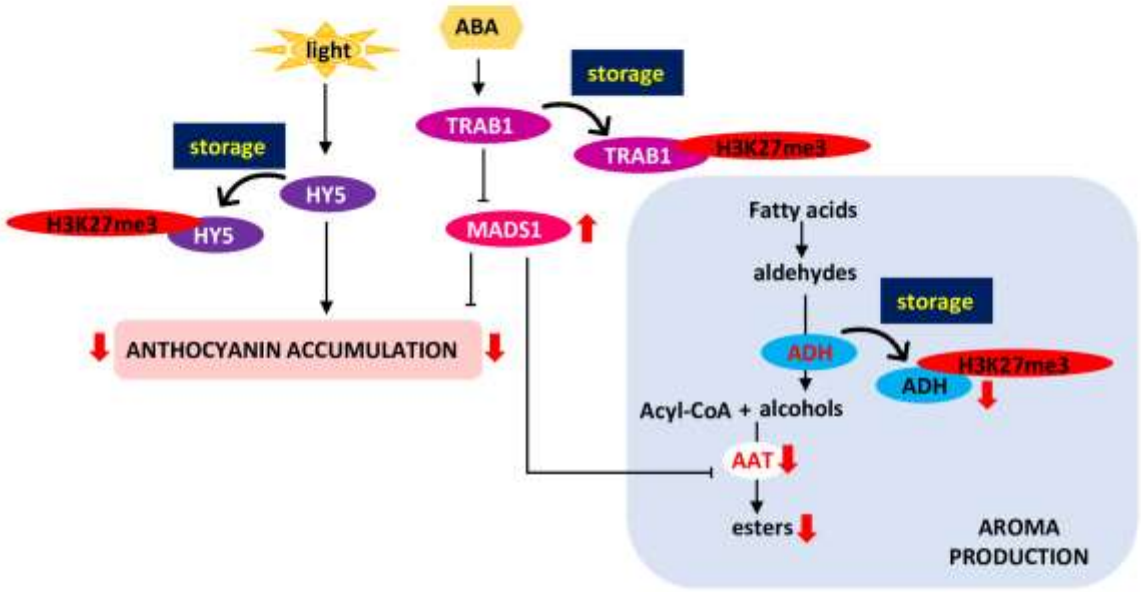

Figure 5. Model showing H3K27me3 regulation of fruit metabolism during storage. Cold dark storage of ripe strawberry fruit results in repression of *FaHY5* transcription through the H3K27me3 mark. This reduces anthocyanin accumulation. Storage also represses FaTRAB1 through the H3K27me3 mark resulting in increased FaMADS1 expression which allows it to repress anthocyanin biosynthesis as well. An increase in MADS1 expression also represses AAT resulting in reduced ester production. ADH is also regulated by the H3K27me3 mark during storage resulting in reduced substrate for AAT, thus also contributing to repression of aroma development.